EUROPEAN ORGANIZATION FOR NUCLEAR RESEARCH

CERN–PPE/93–220

16 December 1993

Measurement of the $B^0 - \overline{B^0}$ Mixing using the Average Electric Charge of Hadron-Jets in Z^0 -Decays

DELPHI Collaboration

Abstract

From the data recorded with the DELPHI detector at LEP in the years 1991-1992, 46497 events were selected having a high-momentum muon in hadron jets. A fit to the average electric charge sum of the jets recoiling against a b-quark jet tagged by a high-P_T muon results in an average mixing parameter of $\overline{\chi} = 0.144 \pm 0.014(stat.)^{+0.017}_{-0.011}(syst.)$.

(To be submitted to Phys. Lett. B)

P.Abreu[20], W.Adam[7], T.Adye[37], E.Agasi[30], I.Ajinenko[43], R.Aleksan[39], G.D.Alekseev[14], A.Algeri[13], P.Allport[21], S.Almehed[23], S.J.Alvsvaag[4], U.Amaldi[7], A.Andreazza[27], P.Antilogus[24], W-D.Apel[15], R.J.Apsimon[37], Y.Arnoud[39], B.Åsman[45], J-E.Augustin[18], A.Augustinus[30], P.Baillon[7], P.Bambade[18], F.Barao[20], R.Barate[12], G.Barbiellini[47], D.Y.Bardin[14], G.J.Barker[34], A.Baroncelli[41], O.Barring[7], J.A.Barrio[25], W.Bartl[50], M.J.Bates[37], M.Battaglia[13], M.Baubillier[22], K-H.Becks[52], M.Begalli[36], P.Beilliere[6], Yu.Belokopytov[43], P.Beltran[9], A.C.Benvenuti[5], M.Berggren[18], D.Bertrand[2], F.Bianchi[46], M.Bigi[46], M.S.Bilenky[14], P.Billoir[22], J.Bjarne[23], D.Bloch[8], J.Blocki[51], S.Blyth[34], V.Bocci[38], P.N.Bogolubov[14], T.Bolognese[39], M.Bonesini[27], W.Bonivento[27], P.S.L.Booth[21], G.Borisov[43], H.Borner[7], C.Bosio[41], B.Bostjancic[44], S.Bosworth[34], O.Botner[48], B.Bouquet[18], C.Bourdarios[18], T.J.V.Bowcock[21], M.Bozzo[11], S.Braibant[2], P.Branchini[41], K.D.Brand[35], R.A.Brenner[7], H.Briand[22], C.Bricman[2], L.Brillault[22], R.C.A.Brown[7], P.Bruckman[16], J-M.Brunet[6], A.Budziak[16], L.Bugge[32], T.Buran[32], H.Burmeister[7], A.Buys[7], J.A.M.A.Buytaert[7], M.Caccia[27], M.Calvi[27], A.J.Camacho Rozas[42], R.Campion[21], T.Camporesi[7], V.Canale[38], K.Cankocak[45], F.Cao[2], F.Carena[7], L.Carroll[21], C.Caso[11], M.V.Castillo Gimenez[49], A.Cattai[7], F.R.Cavallo[5], L.Cerrito[38], V.Chabaud[7], A.Chan[1], M.Chapkin[43], Ph.Charpentier[7], J.Chauveau[22], P.Checchia[35], G.A.Chelkov[14], L.Chevalier[39], P.Chliapnikov[43], V.Chorowicz[22], J.T.M.Chrin[49], V.Cindro[44], P.Collins[34], J.L.Contreras[18], R.Contri[11], E.Cortina[49], G.Cosme[18], F.Couchot[18], H.B.Crawley[1], D.Crennell[37], G.Crosetti[11], J.Cuevas Maestro[33], S.Czellar[13], E.Dahl-Jensen[28], J.Dahm[52], B.Dalmagne[18], M.Dam[32], G.Damgaard[28], E.Daubie[2], A.Daum[15], P.D.Dauncey[7], M.Davenport[7], J.Davies[21], W.Da Silva[22], C.Defoix[6], P.Delpierre[26], N.Demaria[46], A.De Angelis[7], H.De Boeck[2], W.De Boer[15], S.De Brabandere[2], C.De Clercq[2], M.D.M.De Fez Laso[49], C.De La Vaissiere[22], B.De Lotto[47], A.De Min[27], H.Dijkstra[7], L.Di Ciaccio[38], F.Djama[8], J.Dolbeau[6], M.Donszelmann[7], K.Doroba[51], M.Dracos[8], J.Drees[52], M.Dris[31], Y.Dufour[7], F.Dupont[12], D.Edsall[1], L-O.Eek[48], P.A.-M.Eerola[7], R.Ehret[15], T.Ekelof[48], G.Ekspong[45], A.Elliot Peisert[7], M.Elsing[52], J-P.Engel[8], N.Ershaidat[22], M.Espirito Santo[20], D.Fassouliotis[31], M.Feindt[7], A.Ferrer[49], T.A.Filippas[31], A.Firestone[1], H.Foeth[7], E.Fokitis[31], F.Fontanelli[11], K.A.J.Forbes[21], J-L.Fousset[26], S.Francon[24], B.Franek[37], P.Frenkiel[6], D.C.Fries[15], A.G.Frodesen[4], R.Fruhwirth[50], F.Fulda-Quenzer[18], H.Furstenau[15], J.Fuster[7], D.Gamba[46], M.Gandelman[17], C.Garcia[49], J.Garcia[42], C.Gaspar[7], U.Gasparini[35], Ph.Gavillet[7], E.N.Gazis[31], J-P.Gerber[8], P.Giacomelli[7], D.Gillespie[7], R.Gokieli[51], B.Golob[44], V.M.Golovatyuk[14], J.J.Gomez Y Cadenas[7], G.Gopal[37], L.Gorn[1], M.Gorski[51], V.Gracco[11], A.Grant[7], F.Grard[2], E.Graziani[41], G.Grosdidier[18], E.Gross[7], B.Grossetete[22], P.Gunnarsson[45], J.Guy[37], U.Haedinger[15], F.Hahn[52], M.Hahn[45], S.Hahn[52], S.Haider[30], Z.Hajduk[16], A.Hakansson[23], A.Hallgren[48], K.Hamacher[52], G.Hamel De Monchenault[39], W.Hao[30], F.J.Harris[34], V.Hedberg[23], T.Henkes[7], R.Henriques[20], J.J.Hernandez[49], J.A.Hernando[49], P.Herquet[2], H.Herr[7], T.L.Hessing[21], I.Hietanen[13], C.O.Higgins[21], E.Higon[49], H.J.Hilke[7], T.S.Hill[1], S.D.Hodgson[34], T.Hofmokl[51], S-O.Holmgren[45], P.J.Holt[34], D.Holthuizen[30], P.F.Honore[6], M.Houlden[21], J.Hrubec[50], K.Huet[2], K.Hultqvist[45], P.Ioannou[3], P-S.Iversen[4], J.N.Jackson[21], R.Jacobsson[45], P.Jalocha[16], G.Jarlskog[23], P.Jarry[39], B.Jean-Marie[18], E.K.Johansson[45], M.Jonker[7], L.Jonsson[23], P.Juillot[8], G.Kalkanis[3], G.Kalmus[37], F.Kapusta[22], M.Karlsson[45], E.Karvelas[9], S.Katsanevas[3], E.C.Katsoufis[31], R.Keranen[7], B.A.Khomenko[14], N.N.Khovanski[14], B.King[21], N.J.Kjaer[7], H.Klein[7], A.Klovning[4], P.Kluit[30], A.Koch-Mehrin[52], J.H.Koehne[15], B.Koene[30], P.Kokkinias[9], M.Koratzinos[32], K.Korcyl[16], A.V.Korytov[14], V.Kostioukhine[43], C.Kourkoumelis[3], O.Kouznetsov[14], P.H.Kramer[52], M.Krammer[50], C.Kreuter[15], J.Krolikowski[51], I.Kronkvist[23], W.Krupinski[16], W.Kucewicz[16], K.Kulka[48], K.Kurvinen[13], C.Lacasta[49], C.Lambropoulos[9], J.W.Lamsa[1], L.Lanceri[47], P.Langefeld[52], V.Lapin[43], I.Last[21], J-P.Laugier[39], R.Lauhakangas[13], F.Ledroit[12], R.Leitner[29], Y.Lemoigne[39], J.Lemonne[2], G.Lenzen[52], V.Lepeltier[18], J.M.Levy[8], E.Lieb[52], D.Liko[50], J.Lindgren[13], R.Lindner[52], A.Lipniacka[18], I.Lippi[35], B.Loerstad[23], M.Lokajicek[10], J.G.Loken[34], A.Lopez-Fernandez[7], M.A.Lopez Aguera[42], M.Los[30], D.Loukas[9], J.J.Lozano[49], P.Lutz[6], L.Lyons[34], G.Maehlum[32], J.Maillard[6], A.Maio[20], A.Maltezos[9], F.Mandl[50], J.Marco[42], M.Margoni[35], J-C.Marin[7], C.Mariotti[41], A.Markou[9], T.Maron[52], S.Marti[49], C.Martinez-Rivero[42], F.Martinez-Vidal[49], F.Matorras[42], C.Matteuzzi[27], G.Matthiae[38], M.Mazzucato[35], M.Mc Cubbin[21], R.Mc Kay[1], R.Mc Nulty[21], J.Medbo[48], C.Meroni[27], W.T.Meyer[1], M.Michelotto[35], I.Mikulec[50], L.Mirabito[24], W.A.Mitaroff[50], G.V.Mitselmakher[14], U.Mjoernmark[23], T.Moa[45], R.Moeller[28], K.Moenig[7], M.R.Monge[11], P.Morettini[11], H.Mueller[15], W.J.Murray[37], B.Muryn[16], G.Myatt[34], F.Naraghi[12], F.L.Navarria[5], P.Negri[27], S.Nemecek[10], W.Neumann[52], N.Neumeister[50], R.Nicolaidou[3], B.S.Nielsen[28], V.Nikolaenko[43], P.E.S.Nilsen[4], P.Niss[45], A.Nomerotski[35], M.Novak[10], V.Obraztsov[43], A.G.Olshevski[14], R.Orava[13], A.Ostankov[43], K.Osterberg[13], A.Ouraou[39], P.Paganini[18], M.Paganoni[27], R.Pain[22], H.Palka[16], Th.D.Papadopoulou[31], L.Pape[7], F.Parodi[11], A.Passeri[41], M.Pegoraro[35], J.Pennanen[13], L.Peralta[20], H.Pernegger[50], M.Pernicka[50], A.Perrotta[5], C.Petridou[47], A.Petrolini[11], G.Piana[11], F.Pierre[39], M.Pimenta[20], S.Plaszczynski[18], O.Podobrin[15], M.E.Pol[17], G.Polok[16], P.Poropat[47], V.Pozdniakov[14], M.Prest[47], P.Privitera[38], A.Pullia[27], D.Radojicic[34], S.Ragazzi[27], H.Rahmani[31], P.N.Ratoff[19], A.L.Read[32], M.Reale[52], P.Rebecchi[18], N.G.Redaelli[27], M.Regler[50], D.Reid[7], P.B.Renton[34], L.K.Resvanis[3], F.Richard[18], J.Richardson[21], J.Ridky[10], G.Rinaudo[46], A.Romero[46], I.Roncagliolo[11], P.Ronchese[35], C.Ronnqvist[13], E.I.Rosenberg[1], E.Rosso[7], P.Roudeau[18], T.Rovelli[5],

W.Ruckstuhl[30], V.Ruhlmann-Kleider[39], A.Ruiz[42], H.Saarikko[13], Y.Sacquin[39], G.Sajot[12], J.Salt[49], J.Sanchez[25], M.Sannino[11,40], S.Schael[7], H.Schneider[15], M.A.E.Schyns[52], G.Sciolla[46], F.Scuri[47], A.M.Segar[34], A.Seitz[15], R.Sekulin[37], M.Sessa[47], R.Seufert[15], R.C.Shellard[36], I.Siccama[30], P.Siegrist[39], S.Simonetti[11], F.Simonetto[35], A.N.Sisakian[14], G.Skjevling[32], G.Smadja[39,24], N.Smirnov[43], O.Smirnova[14], G.R.Smith[37], R.Sosnowski[51], D.Souza-Santos[36], T.Spassov[20], E.Spiriti[41], S.Squarcia[11], H.Staeck[52], C.Stanescu[41], S.Stapnes[32], G.Stavropoulos[9], F.Stichelbaut[2], A.Stocchi[18], J.Strauss[50], J.Straver[7], R.Strub[8], B.Stugu[4], M.Szczekowski[7], M.Szeptycka[51], P.Szymanski[51], T.Tabarelli[27], O.Tchikilev[43], G.E.Theodosiou[9], A.Tilquin[26], J.Timmermans[30], V.G.Timofeev[14], L.G.Tkatchev[14], T.Todorov[8], D.Z.Toet[30], O.Toker[13], A.Tomaradze[2], B.Tome[20], E.Torassa[46], L.Tortora[41], D.Treille[7], W.Trischuk[7], G.Tristram[6], C.Troncon[27], A.Tsirou[7], E.N.Tsyganov[14], M-L.Turluer[39], T.Tuuva[13], I.A.Tyapkin[22], M.Tyndel[37], S.Tzamarias[21], B.Ueberschaer[52], S.Ueberschaer[52], O.Ullaland[7], V.Uvarov[43], G.Valenti[5], E.Vallazza[7], J.A.Valls Ferrer[49], C.Vander Velde[2], G.W.Van Apeldoorn[30], P.Van Dam[30], M.Van Der Heijden[30], W.K.Van Doninck[2], J.Van Eldik[30], P.Vaz[7], G.Vegni[27], L.Ventura[35], W.Venus[37], F.Verbeure[2], M.Verlato[35], L.S.Vertogradov[14], D.Vilanova[39], P.Vincent[24], L.Vitale[47], E.Vlasov[43], A.S.Vodopyanov[14], M.Vollmer[52], M.Voutilainen[13], V.Vrba[41], H.Wahlen[52], C.Walck[45], F.Waldner[47], A.Wehr[52], M.Weierstall[52], P.Weilhammer[7], A.M.Wetherell[7], J.H.Wickens[2], M.Wielers[15], G.R.Wilkinson[34], W.S.C.Williams[34], M.Winter[8], G.Wormser[18], K.Woschnagg[48], A.Zaitsev[43], A.Zalewska[16], D.Zavrtanik[44], E.Zevgolatakos[9], N.I.Zimin[14], M.Zito[39], D.Zontar[44], R.Zuberi[34], G.Zumerle[35], J.Zuniga[49]

[1] Ames Laboratory and Department of Physics, Iowa State University, Ames IA 50011, USA
[2] Physics Department, Univ. Instelling Antwerpen, Universiteitsplein 1, B-2610 Wilrijk, Belgium
and IIHE, ULB-VUB, Pleinlaan 2, B-1050 Brussels, Belgium
and Faculté des Sciences, Univ. de l'Etat Mons, Av. Maistriau 19, B-7000 Mons, Belgium
[3] Physics Laboratory, University of Athens, Solonos Str. 104, GR-10680 Athens, Greece
[4] Department of Physics, University of Bergen, Allégaten 55, N-5007 Bergen, Norway
[5] Dipartimento di Fisica, Università di Bologna and INFN, Via Irnerio 46, I-40126 Bologna, Italy
[6] Collège de France, Lab. de Physique Corpusculaire, IN2P3-CNRS, F-75231 Paris Cedex 05, France
[7] CERN, CH-1211 Geneva 23, Switzerland
[8] Centre de Recherche Nucléaire, IN2P3 - CNRS/ULP - BP20, F-67037 Strasbourg Cedex, France
[9] Institute of Nuclear Physics, N.C.S.R. Demokritos, P.O. Box 60228, GR-15310 Athens, Greece
[10] FZU, Inst. of Physics of the C.A.S. High Energy Physics Division, Na Slovance 2, CS-180 40, Praha 8, Czechoslovakia
[11] Dipartimento di Fisica, Università di Genova and INFN, Via Dodecaneso 33, I-16146 Genova, Italy
[12] Institut des Sciences Nucléaires, IN2P3-CNRS, Université de Grenoble 1, F-38026 Grenoble, France
[13] Research Institute for High Energy Physics, SEFT, P.O. Box 9, FIN-00014 University of Helsinki, Finland
[14] Joint Institute for Nuclear Research, Dubna, Head Post Office, P.O. Box 79, 101 000 Moscow, Russian Federation
[15] Institut für Experimentelle Kernphysik, Universität Karlsruhe, Postfach 6980, D-76128 Karlsruhe, Germany
[16] High Energy Physics Laboratory, Institute of Nuclear Physics, Ul. Kawiory 26a, PL-30055 Krakow 30, Poland
[17] Centro Brasileiro de Pesquisas Físicas, rua Xavier Sigaud 150, RJ-22290 Rio de Janeiro, Brazil
[18] Université de Paris-Sud, Lab. de l'Accélérateur Linéaire, IN2P3-CNRS, Bat 200, F-91405 Orsay, France
[19] School of Physics and Materials, University of Lancaster, GB-Lancaster LA1 4YB, UK
[20] LIP, IST, FCUL - Av. Elias Garcia, 14-1°, P-1000 Lisboa Codex, Portugal
[21] Department of Physics, University of Liverpool, P.O. Box 147, GB-Liverpool L69 3BX, UK
[22] LPNHE, IN2P3-CNRS, Universités Paris VI et VII, Tour 33 (RdC), 4 place Jussieu, F-75252 Paris Cedex 05, France
[23] Department of Physics, University of Lund, Sölvegatan 14, S-22363 Lund, Sweden
[24] Université Claude Bernard de Lyon, IPNL, IN2P3-CNRS, F-69622 Villeurbanne Cedex, France
[25] Universidad Complutense, Avda. Complutense s/n, E-28040 Madrid, Spain
[26] Univ. d'Aix - Marseille II - CPP, IN2P3-CNRS, F-13288 Marseille Cedex 09, France
[27] Dipartimento di Fisica, Università di Milano and INFN, Via Celoria 16, I-20133 Milan, Italy
[28] Niels Bohr Institute, Blegdamsvej 17, DK-2100 Copenhagen 0, Denmark
[29] NC, Nuclear Centre of MFF, Charles University, Areal MFF, V Holesovickach 2, CS-180 00, Praha 8, Czechoslovakia
[30] NIKHEF-H, Postbus 41882, NL-1009 DB Amsterdam, The Netherlands
[31] National Technical University, Physics Department, Zografou Campus, GR-15773 Athens, Greece
[32] Physics Department, University of Oslo, Blindern, N-1000 Oslo 3, Norway
[33] Dpto. Fisica, Univ. Oviedo, C/P.Jimenez Casas, S/N-33006 Oviedo, Spain
[34] Department of Physics, University of Oxford, Keble Road, Oxford OX1 3RH, UK
[35] Dipartimento di Fisica, Università di Padova and INFN, Via Marzolo 8, I-35131 Padua, Italy
[36] Depto. de Fisica, Pontificia Univ. Católica, C.P. 38071 RJ-22453 Rio de Janeiro, Brazil
[37] Rutherford Appleton Laboratory, Chilton, GB - Didcot OX11 OQX, UK
[38] Dipartimento di Fisica, Università di Roma II and INFN, Tor Vergata, I-00173 Rome, Italy
[39] Centre d'Etude de Saclay, DSM/DAPNIA, F-91191 Gif-sur-Yvette Cedex, France
[40] Dipartimento di Fisica-Università di Salerno, I-84100 Salerno, Italy
[41] Istituto Superiore di Sanità, Ist. Naz. di Fisica Nucl. (INFN), Viale Regina Elena 299, I-00161 Rome, Italy
[42] C.E.A.F.M., C.S.I.C. - Univ. Cantabria, Avda. los Castros, S/N-39006 Santander, Spain
[43] Inst. for High Energy Physics, Serpukov P.O. Box 35, Protvino, (Moscow Region), Russian Federation
[44] J. Stefan Institute and Department of Physics, University of Ljubljana, Jamova 39, SI-61000 Ljubljana, Slovenia
[45] Fysikum, Stockholm University, Box 6730, S-113 85 Stockholm, Sweden
[46] Dipartimento di Fisica Sperimentale, Università di Torino and INFN, Via P. Giuria 1, I-10125 Turin, Italy
[47] Dipartimento di Fisica, Università di Trieste and INFN, Via A. Valerio 2, I-34127 Trieste, Italy
and Istituto di Fisica, Università di Udine, I-33100 Udine, Italy
[48] Department of Radiation Sciences, University of Uppsala, P.O. Box 535, S-751 21 Uppsala, Sweden
[49] IFIC, Valencia-CSIC, and D.F.A,M.N., U. de Valencia, Avda. Dr. Moliner 50, E-46100 Burjassot (Valencia), Spain
[50] Institut für Hochenergiephysik, Österr. Akad. d. Wissensch., Nikolsdorfergasse 18, A-1050 Vienna, Austria
[51] Inst. Nuclear Studies and University of Warsaw, Ul. Hoza 69, PL-00681 Warsaw, Poland
[52] Fachbereich Physik, University of Wuppertal, Postfach 100 127, D-5600 Wuppertal 1, Germany

Introduction

The neutral mesons B_d^0 ($\overline{b}d$) and B_s^0 ($\overline{b}s$) physically are quantum mechanical mixtures of the beauty eigenstates $|B^0>$ and $|\overline{B^0}>$ evolving in time as an oscillation between the two. This effect was first measured in 1987 [1]. The $\Delta_B = 2$ transition is a second order weak interaction as shown in figure 1. In the Standard Model the transition amplitude [2] depends on the fundamental parameters m_{top}, and the two CKM matrix-elements [3] V_{td} and V_{ts}.

The observable of mixing is the probability that a B^0 meson which is produced as a $|B^0>$ decays as its antiparticle,

$$\chi_d = \frac{B_d^0 \to \overline{B_d^0} \to final}{all \quad B_d^0} \qquad \chi_s = \frac{B_s^0 \to \overline{B_s^0} \to final}{all \quad B_s^0}. \tag{1}$$

At LEP the B hadrons are thought to be formed independently during the fragmentation phase subsequent to a Z^0 decay into a $b\overline{b}$ pair. A (model dependent) pair creation mechanism of new $q\overline{q}$ pairs within the colour interaction field allows the leading b quark to pick up an antiquark ($\overline{u}$,$\overline{d}$,$\overline{s}$) from the vacuum forming a charged B meson ($b\overline{u}$), or one of the B^0 mesons ($b\overline{d}$ and $b\overline{s}$). The probabilities for these processes are called f_u, f_d and f_s. Baryon formation occurs in a further fraction f_{baryon} [†] of the events. Without differentiating between B_d^0 and B_s^0 mesons one measures a linear combination of the mixing parameters

$$\overline{\chi} = a \cdot \chi_d + b \cdot \chi_s \tag{2}$$

a and b being coefficients representing the abundance and sensitivity of the B^0 type to the observable. The most common method [4] to measure the probability $\overline{\chi}$ is based upon events with a dilepton topology i.e. a situation in which both B hadrons in the event decay semi-leptonically. Both the semi-leptonic decays of the B_d^0 and the B_s^0 yield a positively charged lepton but mixing will flip the charge of the lepton for both the strange and the non-strange B^0s. Thus in a dilepton analysis, assuming the semi-leptonic branching ratios of both B^0s to be equal, a and b simply represent the abundance of the corresponding B^0 in b fragmentation: $a = f_d,\ b = f_s$.

Determining the beauty of the jets from the charge of the two leptons results in a small efficiency, since only about 20% of all B hadrons decay semi-leptonically. In order to use ten times the statistics (five times if only muons are used) the approach of this letter is to obtain the charge of the beauty quark on one side of the event from a semi-leptonic decay (thereby also tagging a b event) and analyse the opposite hemisphere by means of a momentum weighted charge sum (jet charge). As a consequence of the fact that $B^0 - \overline{B^0}$ transitions break the deterministic relation between the beauty on the lepton side and on the jet side, mixing tends to lower the (absolute) value of the average jet charge opposite to leptons of a given charge. The quantitative analysis relies on the expectation for the b jet charge obtained from a detailed Monte Carlo simulation which reveals that χ_s affects the jet charge less than χ_d. Therefore the parameters of the linear combination in eqn. 2 deviate from the dilepton case. It has been proposed [5] to write $a = f_d$ and $b = C \cdot f_s$.

[†] The following relations between the parameters f are given: $f_u = f_d$, $f_s = x_{\frac{s}{u}} f_u$ where $x_{\frac{s}{u}}$ is called the s quark suppression factor. No heavy flavour production during the fragmentation is assumed, $f_c = f_b = 0$ and thus $f_u + f_d + f_s + f_{baryon} = 1$.

The DELPHI Detector and Event Selection

The DELPHI detector at LEP has been described in detail [6]. This analysis is mainly based upon charged particle reconstruction and muon identification. Charged particles were measured using the tracking system consisting of a vertex-detector of three layers of silicon microstrip diodes, an inner jet-chamber, a time projection chamber (TPC) and additional drift chambers in the barrel and forward region which frame the barrel and forward ring imaging Čerenkov counter systems. All are installed inside a superconducting coil. Muons were identified using drift chambers which are installed in the outer layers and on the surface of the hadron calorimeter in combination with the central tracking system [7]. Neutral particles were accepted as unlinked calorimetric showers of reconstructed energy above 2 GeV which lay inside the polar angle region of $|\cos\theta| < 0.75$.

Charged particle tracks were required to have a minimum length of 50 cm and a maximum impact parameter at the interaction point of 5 cm in r and 10 cm in z, r denoting the distance from the interaction point (IP) in a plane perpendicular to the beam line and z the distance from the IP along the beam. The track polar angle was required to lie inside $|\cos\theta| < 0.92$. Accepted charged particles were required to have a momentum above 0.1 GeV/c.

Multihadronic events were expected to have at least three charged particles in each z hemisphere amounting to a total absolute momentum in charged particles of at least 15 GeV/c. The event sphericity axis was required to lie within a polar angle range of $|\cos\theta| < 0.95$. Jets were reconstructed using the LUCLUS algorithm with default clustering parameter ($d_{join} = 2.5$). Muons were identified in the region of polar angles down to 11 degrees. The events were retained if at least one muon of momentum between 3.0 and 35.0 GeV/c and with momentum transverse to the momentum sum of the other particles of the jet, P_T between 0.5 and 7.5 GeV/c, was detected. Starting from about 970000 multihadronic Z^0 decays recorded during the 1991 and 1992 runs of DELPHI, these requirements led to a sample of 46497 hadronic events with a muon in a jet. A sample of 496324 $Z^0 \to q\overline{q}$ Monte Carlo events was generated with the JETSET 7.3 [8] program using the parton shower model together with string fragmentation in hybrid mode, i.e. the Lund symmetric fragmentation function for light quarks and Peterson's function for c and b quarks.

The decay of heavy quarks proceed in JETSET via a free quark decay model which describes the inclusive lepton spectrum quite well. But the lepton spectrum from $B \to Dl\nu$ decays is too soft in JETSET and the lepton spectrum from $B \to D^* l\nu$ decay modes is too hard. Therefore the calculation of the weak matrix elements for the decays of heavy flavours have been modified in the DELPHI Monte Carlo simulation. The matrix elements for the B and D meson decays to $X(e,\mu)\ \nu$ are calculated following the predictions of Grinstein, Isgur, Scora and Wise [9] and the decays $B \to X\tau\nu$ according to the model developed by Wirbel, Stech, Bauer [10]. The lepton spectra from B meson decays as predicted in these form-factor models are in excellent agreement with the experimental data [11]. For the decay $B \to D^{**}(e,\mu)\ \nu$ a branching fraction of 2% was assumed.

The Monte Carlo event sample was passed through a detailed detector simulation and analysed in the same way as the data, yielding 23004 hadronic Z^0 decays with an identified muon. The resulting lepton spectra (P and P_T) are plotted together with the measured data in figure 2.

Analysis Method

In Z^0 decays beauty is usually produced in a pair of quark and anti-quark recoiling from each other. This defines a two jet structure in the event topology. The total beauty in the event at the time of production is zero. Therefore the analysis of B^0 mixing is based upon the measurement of the total beauty when the b quarks decay.

On one side of the event this is done by measuring the charge of a high momentum muon from a semi-leptonic b decay. The beauty in the opposite hemisphere is evaluated from the (longitudinal) momentum weighted charge sum Q^{oppo},

$$Q^{oppo} = \frac{\sum_i q_i \cdot |\vec{p_i} \cdot \vec{e_S}|^\kappa}{\sum_i |\vec{p_i} \cdot \vec{e_S}|^\kappa}. \tag{3}$$

The sum runs over all charged tracks with a momentum above 0.2 GeV/c in the hemisphere, experimentally defined by the sphericity axis (unit vector $\vec{e_S}$), opposite to the high momentum muon. The parameter κ gives different weights to the hard and soft parts of the momentum spectrum. The statistical precision of the Monte Carlo prediction of $< Q^{oppo} >$ depends on the r.m.s. of the jet charge distribution and this r.m.s. rises with κ. On the other hand too low a value of κ overemphasizes the lowest momenta and reduces the sensitivity to the charge of the heavy quark in the B meson to which the jet belongs. It was found that a value of $\kappa = 0.6$ minimizes the statistical error of the final result.

The jet charge Q^{oppo} in a single event is not a unique and unambiguous measure of the b quark charge like the lepton charge in the semi-leptonic final state. Nevertheless, due to the *leading particle effect* (i.e. the experimental fact that the most energetic particle in a jet tends to carry the original heavy quark [12]) the B hadron receives a large fraction of the quark's momentum which is transferred to its decay products. This establishes a correlation between the jet charge and the beauty of the jet. The mean of the jet charge distribution $< Q^{oppo} >$ will emerge as a unique and unambiguous function of the b charge in a large sample of b-jets.

Due to mixing on the lepton side, the sample of jets opposite to a lepton of a fixed charge sign (e.g. positive) will contain a relative fraction of $\beta = f_d \cdot \chi_d + f_s \cdot \chi_s$ which belong to this event set just because the lepton charge is reversed. This fraction of events will have a $\overline{b}$-jet instead of a b-jet opposite the positive lepton. Ignoring all backgrounds and assuming the semi-leptonic branching ratios of all B mesons to be equal, one expects for the average jet charge

$$< Q^{oppo} > = (1-\beta) < Q_{b-jet} > + \beta < Q_{\overline{b}-jet} > . \tag{4}$$

The above equation is not complete because of the fact that the mixing affects the average b-jet charge as well, tending to reduce the difference between b- and $\overline{b}$-jet, thereby reducing the sensitivity of the method. The expectation for the mixing dependent b-jet charge is composed of five terms,

$$\begin{aligned} < Q_{b-jet}(\chi_d, \chi_s) > \; = \; & (f_{b-Baryon} + f_u) < Q(\Lambda_b, B^-) > + \\ & f_d(1-\chi_d) < Q(\overline{B^0_d}) > + f_d\chi_d < Q(\overline{B^0_d} \to B^0_d) > + \\ & f_s(1-\chi_s) < Q(\overline{B^0_s}) > + f_s\chi_s < Q(\overline{B^0_s} \to B^0_s) > . \end{aligned} \tag{5}$$

In the above formula $< Q(\Lambda_b, B^-) >$ represents the average jet charge of all b-jets in which the b quark finds itself inside a B hadron that is unable to undergo a transition into its antiparticle, $< Q(\overline{B^0}) >$ denotes the jet charge for jets in which the $\overline{B^0}$ decays

as it was produced, while $< Q(\overline{B^0} \rightarrow B^0) >$ is the jet charge for jets in which a $\overline{B^0}$ was produced, which subsequently decays as its anti-particle. The different contributions to $< Q_{b-jet} >$ were obtained from a Monte Carlo simulation and are listed in table 1. Note that to improve the statistical accuracy of the Monte Carlo model equal fractions of normal B^0 decays and $B^0 \rightarrow \overline{B^0}$ decays are desirable. Therefore the generator level runs of the JETSET program were performed with full mixing of both B_d^0 and B_s^0. Inserting eqn. 5 into eqn. 4 yields the function generating the expected value of $< Q^{oppo} >$ for a pure sample of primary semi-leptonic b decays including the decays from the $b \rightarrow \tau \rightarrow \mu$ cascade (subscript bp in eqn. 6). However, various background reactions have to be considered and introduced into the model. Here the importance of the P_T spectrum of the muons becomes evident since the relative contributions of the background classes change with P_T.

Calling $a_{class}^{(i)}$ the relative abundance of the different classes in the P_T bin, i, and $< Q_{class} >$ the Monte-Carlo determined average jet charge in each class, the complete expression for the jet charge opposite to a sample of positive muons is

$$\begin{aligned} Q^{oppo}(\chi_d,\chi_s)^{(i)} &= a_{bp}^{(i)} \cdot \{(1-\beta(\chi_d,\chi_s))< Q_{b-jet}(\chi_d,\chi_s) > + \beta(\chi_d,\chi_s)< Q_{\overline{b}-jet}(\chi_d,\chi_s) >\} \\ &+ a_{bc}^{(i)} \cdot \{(1-\tilde{\beta}(\chi_d,\chi_s))< Q_{\overline{b}-jet}(\chi_d,\chi_s) > + \tilde{\beta}(\chi_d,\chi_s)< Q_{b-jet}(\chi_d,\chi_s) >\} \\ &+ a_{cp}^{(i)} \cdot < Q_{\overline{c}-jet} > \\ &+ a_{double-c}^{(i)} \cdot < Q_{double-c} > \\ &+ a_{any\ \mu}^{(i)} \cdot < Q_{any\ \mu} > \\ &+ a_{hadrons}^{(i)} \cdot < Q_{hadrons} > . \end{aligned} \tag{6}$$

A fit to this expression was carried out over a range of 17 P_T bins between 0.5 and 7.5 GeV/c, χ_s was fixed while χ_d was varied.

The model expectation for a muon from a semi-leptonic decay of a charmed hadron from the b-c-cascade (bc) is in principle obtained from the equations 4 and 5 by a charge exchange operation [‡]. Primary c decays (cp) will contribute some jets with $< Q^{oppo} > =< Q\ (c-jet) >$, with the lepton charge following from that of the quark. The class 'double charm' comprises all muons from the $b-c$ cascade which come from B decays with two charm quarks in the final state (e.g. J/ψ or two D mesons); here the beauty quantum number of the original B meson does not follow from the muon charge. The class 'any μ' refers to (semi)leptonic decays of light flavoured hadrons and the class 'misidentified hadrons' denotes the contribution of hadron tracks that are erroneously tagged as lepton candidates by the experimental particle identification procedure.

The fit procedure takes advantage of the fact that the fraction of the background classes depends on the transverse momentum of the lepton candidate with the b purity increasing with increasing transverse momentum. In the small fraction of events with more than two b quarks (four jets) only the decays of the two B hadrons with the highest momenta were included in this analysis.

The total charge sum of a Z^0 decay is zero. However, the measured total charge may be different. Due to secondary hadronic interactions the total particle charge is increased since hadrons interact preferentially with positively charged nuclear matter.

This leads to an excess of positive particles,

$$\frac{N^+ - N^-}{N^+ + N^-} = 0.0100 \pm 0.0006\ (data)$$

[‡]Due to different semi-leptonic branching ratios of charged and neutral D mesons the probability to find a $B^{\pm}$-jet in the b-c-cascade lepton sample is suppressed. This is expressed by $\tilde{\beta}(\chi_d,\chi_s)$ in eqn. 6.

	generator level		full detect or simulation	
	Q_{b-jet}	$Q_{\overline{b}-jet}$	Q_{b-jet}	$Q_{\overline{b}-jet}$
$< Q(\Lambda_b, B^-) >$	-0.101 ± 0.001	$+0.100 \pm 0.001$	-0.101 ± 0.004	$+0.100 \pm 0.004$
$< Q(\overline{B_s^0})) >$	-0.045 ± 0.003	$+0.047 \pm 0.003$	-0.064 ± 0.010	$+0.058 \pm 0.011$
$< Q(\overline{B_s^0} \to B_s^0)) >$	-0.027 ± 0.003	$+0.027 \pm 0.003$	-0.006 ± 0.011	$+0.023 \pm 0.011$
$< Q(\overline{B_d^0})) >$	-0.091 ± 0.002	$+0.090 \pm 0.002$	-0.083 ± 0.005	$+0.075 \pm 0.005$
$< Q(\overline{B_d^0} \to B_d^0)) >$	$+0.022 \pm 0.002$	-0.022 ± 0.002	$+0.009 \pm 0.009$	-0.026 ± 0.011
total $< Q >$	-0.068 ± 0.001	$+0.071 \pm 0.001$	-0.080 ± 0.003	$+0.076 \pm 0.003$

Table 1: The average b-jet charge ($\kappa = 0.6$) determined from a Monte Carlo study. Only the last line depends on the mixing chosen. Values are $(\chi_d, \chi_s) = (0.49, 0.49)$ for the generator and $(\chi_d, \chi_s) = (0.18, 0.49)$ for the full detector simulation.

$$= \quad 0.0130 \pm 0.0008 \ (simulation) \tag{7}$$

A related observable is the ratio of negative over positive particles as a function of the momentum which is shown in figure 3 for the data.

A weighting technique was applied to compensate for the positive charge excess. During the computation of Q^{oppo} the charge of positive particles is weighted by the parametrisation function $f(p) = 1 - (c_1 + c_2 p + c_3 p^2) exp(-c_4 p) - c_5$. Note that this procedure does not rely on the simulation. For the Monte Carlo events a similar procedure was applied and an independent set of parameters was obtained. [§]

Result

The spectra of Q^{oppo} for the positive and negative muon samples are displayed in figure 4. The mean values of similar distributions for different bins of muon-P_T are displayed in figure 5. The rise in absolute value of $< Q^{oppo} >$ with increasing P_T is due to the higher b purity at large P_T values of the lepton. There is no other kinematical correlation between the two observables. The solid lines indicate the fit result and the expectations for maximal mixing ($\chi_d = \chi_s = 0.5$) and no mixing ($\chi_d = \chi_s = 0.0$). The hatched band indicates the statistical error of the fitted Monte Carlo model. The data points in figure 5 are given numerically in table 2.

The values for the coefficients $a^{(i)}$ of eqn. 6 were taken from the Monte Carlo description of the P_T spectrum shown in figure 2. The relative sample composition can be found in table 3 while the absolute number of events in each P_T bin is listed in table 4. The Monte Carlo events are subdivided into the different lepton classes.

The Monte Carlo model in eqn. 6 is completed by the determination of the expectation for $< Q^{oppo} >$ for the five b-jet classes (see table 1) and the background classes. The result of the simulation of the non-b background classes is displayed in table 5.

Note that the values in tables 1 and 5 correspond to the composition of a sample of jets with a high P and P_T lepton in the *opposite* hemisphere. As a consequence of this topology the hemispheres which contribute to these values are depleted of lepton candidates while the lepton side obviously is enhanced in muon tracks. Since high momentum muons are

[§] The parameters for the data were $c_1 = -0.046, c_2 = 0.17, c_3 = -0.06, c_4 = 1.3, c_5 = 0.013$ and the description of the MC required $c_1 = -0.046, c_2 = 0.338, c_3 = -0.214, c_4 = 1.487, c_5 = 0.026$.

P_T [GeV/c]	0.5-0.6	0.6-0.7	0.7-0.8	0.8-0.9	0.9-1.0	1.0-1.2
$< Q^{oppo} >(\mu^+)$	$-0.020(6)$	$-0.022(6)$	$-0.016(7)$	$-0.023(7)$	$-0.018(8)$	$-0.030(6)$
$< Q^{oppo} >(\mu^-)$	$+0.022(6)$	$+0.016(6)$	$+0.018(7)$	$+0.027(7)$	$+0.028(8)$	$+0.026(6)$
P_T [GeV/c]	1.2-1.4	1.4-1.6	1.6-1.8	1.8-2.0	2.0-2.4	2.4-2.8
$< Q^{oppo} >(\mu^+)$	$-0.032(6)$	$-0.043(7)$	$-0.038(8)$	$-0.043(8)$	$-0.048(7)$	$-0.038(8)$
$< Q^{oppo} >(\mu^-)$	$+0.044(7)$	$+0.039(7)$	$+0.029(8)$	$+0.042(8)$	$+0.047(7)$	$+0.049(9)$
P_T [GeV/c]	2.8-3.2	3.2-3.6	3.6-4.0	4.0-5.0	5.0-7.5	
$< Q^{oppo} >(\mu^+)$	$-0.062(11)$	$-0.049(13)$	$-0.064(16)$	$-0.034(15)$	$-0.068(20)$	
$< Q^{oppo} >(\mu^-)$	$+0.047(10)$	$+0.038(13)$	$+0.059(16)$	$+0.045(14)$	$-0.054(20)$	

Table 2: The observed value of $< Q^{oppo} >$ in the different P_T bins for positive and negative muons.

full detector simulation	
class	contribution(%)
$b - primary$	40.5 ± 0.4
$b - c - cascade$	10.2 ± 0.2
$b \rightarrow double - c$	2.4 ± 0.1
$c \rightarrow \ lepton$	14.7 ± 0.3
$any\ \mu$	2.9 ± 0.1
$misid.\ hadrons$	29.2 ± 0.4

Table 3: The selected lepton sample composition; the errors are statistical only .

charged tracks they contribute heavily to the jet charge. Using the data, the size of this effect is demonstrated by the analysis of the distribution of the jet charge Q^{same} on the lepton side of the event which is shown in figure 6. The mean value for the jet sample containing positive (negative) muon candidates is $< Q^{same} >= 0.1813 \pm 0.0017$ ($< Q^{same} >= -0.1756 \pm 0.0017$). The corresponding distributions in the Monte Carlo have mean values $< Q^{same} >= 0.1867 \pm 0.0025$ and $< Q^{same} >= -0.1723 \pm 0.0024$. The jet charge distributions containing the lepton candidate are nearly not affected by mixing. Therefore they can be used as powerful check of the Monte Carlo description of the data.

The interpretation of the average jet charge opposite to the lepton candidate has to take into account not only the mixing but also the realistic composition of the jets i.e. the fact that the probability to find a second hard lepton track in the opposite jet is considerably lower ¶ than the fraction of leptons within an unspecified sample of b-jets.

The average jet charge from non-b background, except for charm, is small. This can be understood from the fact that in kaon or pion decays and in the case of misidentified hadrons the charge of the lepton candidate does not follow directly from the flavour of the jet. Thus the reconstruction of $< Q^{oppo} >$ from this source yields approximately zero, indicating a mixture of equal parts of quark and antiquark jets.

Nevertheless, here the leading particle effect gives a slightly higher probability to have positive hadrons misidentified in jets from positive quarks. So the jet charge average of the non-charm background is not *a priori* zero. This could, in principle, establish a small mixing sensitive part in the fraction of misidentified hadrons coming from b decays.

¶If x denotes the probability to find a high momentum lepton in a jet, the fraction of dilepton events within the single-lepton sample is $\frac{x^2}{1-(1-x)^2} = \frac{x}{2-x}$ which is nearly half of x for small x.

P_T [GeV/c]	0.5-0.6	0.6-0.7	0.7-0.8	0.8-0.9	0.9-1.0	1.0-1.2
Data	4787	4387	3780	3404	2953	5110
$b-primary$	198	226	272	354	386	889
$b-c-casc$	312	334	307	237	191	338
$b-double-c$	81	73	92	57	53	49
$c-primary$	549	474	412	340	239	406
$any\ \mu$	156	101	97	79	53	63
$misid.\ hadrons$	1199	993	784	652	552	784
P_T [GeV/c]	1.2-1.4	1.4-1.6	1.6-1.8	1.8-2.0	2.0-2.4	2.4-2.8
Data	4075	3258	2764	2294	3414	2124
$b-primary$	927	906	853	748	1178	844
$b-c-casc$	186	144	81	57	76	44
$b-double-c$	45	28	20	12	16	15
$c-primary$	285	185	122	94	119	55
$any\ \mu$	44	24	19	8	15	3
$misid.\ hadrons$	510	323	223	152	217	111
P_T [GeV/c]	2.8-3.2	3.2-3.6	3.6-4.0	4.0-5.0	5.0-7.5	
Data	1452	882	589	773	451	
$b-primary$	589	311	224	254	154	
$b-c-casc$	15	18	5	6	1	
$b-double-c$	6	5	0	3	6	
$c-primary$	36	29	14	13	13	
$any\ \mu$	1	3	2	0	0	
$misid.\ hadrons$	85	46	31	25	38	

Table 4: The observed P_T distribution comparing the data (first line) with the different classes of muon candidates from the Monte Carlo (subsequent lines) (Figure 2).

However, this is not explicitly included in the fit but this background is taken from the Monte Carlo with the mixing parameters of the simulation (see table 1).

The fit was performed with the following values for the relative contribution to the total b-jet sample:

$$\begin{aligned} F_d &= 0.396 \pm 0.005 \quad F_s = 0.124 \pm 0.003 \quad (b-primary) \\ F_d &= 0.492 \pm 0.012 \quad F_s = 0.100 \pm 0.005 \quad (b-c-cascade) \end{aligned} \tag{8}$$

Starting from the the original Monte Carlo settings $f_d = 0.391$ and $f_s = 0.117$, which follow if one assumes an s quark suppression factor of 0.3 and a baryon contribution of 10%, the fractions F_d and F_s result from the full detector simulation plus event selection (distinguished here with capital letters).

A least squares fit to eqn. 6 was performed in 17 bins of muon transverse momentum. The two samples of positive and negative lepton candidates were treated separately in the data and in the Monte Carlo. In the fit χ_d was allowed to vary while χ_s was fixed, this yielded

$$\begin{aligned} \underline{for\ \chi_s = 0.0:} \quad & \chi_d = 0.391 \pm 0.059\ (\mu^+) \quad \chi_d = 0.354 \pm 0.049\ (\mu^-) \\ \underline{for\ \chi_s = 0.5:} \quad & \chi_d = 0.247 \pm 0.058\ (\mu^+) \quad \chi_d = 0.223 \pm 0.048\ (\mu^-). \end{aligned} \tag{9}$$

	full detector simulation	
class	$< Q >$ *opp. to* μ^+	$< Q >$ *opp. to* μ^-
$c \rightarrow$ *lepton*	-0.071 ± 0.005	$+0.053 \pm 0.005$
any μ	-0.005 ± 0.010	$+0.027 \pm 0.010$
misid. hadrons	-0.012 ± 0.004	$+0.009 \pm 0.004$

Table 5: The average jet charge opposite to non-b background lepton candidates determined from a Monte Carlo study.

parameter	variation range (GeV/c)	standard fit value	$\Delta\overline{\chi}$
P^{min}	$2.0 - 4.0$	3.0	$^{+0.000}_{-0.003}$
P^{max}	$30.0 - 45.0$	35.0	$^{+0.003}_{-0.000}$
P_T^{min}	$0.3 - 0.6$	0.5	$^{+0.004}_{-0.000}$
P_T^{max}	$5.0 - 7.5$	7.5	$^{+0.003}_{-0.000}$
binning	$11 < N_{bin} < 24$	17	± 0.001

Table 6: Systematic studies of the lepton cuts and the binning

The results for other assumptions on the value of χ_s are displayed in figure 7. The width of the error bands represent the total error including the systematic errors. The variation of χ_d with χ_s is almost linear, with slope of -0.272 ± 0.015 (statistical error from the Monte Carlo).

With $C = 0.91 \pm 0.05$, which was obtained from the slope of the plot in figure 7 and the original Monte Carlo settings, the result can be written as

$$\overline{\chi} = f_d \cdot \chi_d + f_s \cdot C \cdot \chi_s = 0.144 \pm 0.014. \tag{10}$$

The error includes the statistical error of the Monte Carlo. The corresponding expectation for $< Q^{oppo} >$ in different P_T bins is displayed in figure 5 together with the observed data.

Systematic Errors

The systematic error on the measurement can be split into two parts following the treatment of the two hemispheres of each event. First, there is the study of the lepton

class	variation range (%)	$\Delta\overline{\chi}$
$b - primary$	± 8	$^{+0.004}_{-0.004}$
$b - c - cascade$	± 15	$^{+0.006}_{-0.004}$
$b \rightarrow double - c$	± 20	$^{+0.001}_{-0.000}$
$c \rightarrow$ *lepton*	± 11	$^{+0.002}_{-0.001}$
any real μ	± 10	$^{+0.001}_{-0.000}$
misid. hadrons	± 7	$^{+0.003}_{-0.002}$

Table 7: Systematic error due to the variation in the lepton sample composition.

Parameter	variation range	standard fit value	$\Delta\overline{\chi}$
ϵ_b	0.004-0.007	0.006	$^{+0.008}_{-0.004}$
ϵ_c / ϵ_b	7-11	9	$^{+0.002}_{-0.001}$
$x_{\frac{s}{u}}$	0.26-0.34	0.3	± 0.005
$f_{baryons}$	0.0-0.2	0.1	± 0.001
Λ^{PS}_{QCD}	0.255-0.400	0.255	$+0.004$
$\frac{vector\ mesons}{all\ mesons}^{c,b}$	0.65-0.85	0.75	± 0.002
σ_{P_T}	0.345-0.445	0.395	$^{+0.005}_{-0.001}$
M_{frag}	1.0-2.0	2.0	-0.005

Table 8: Systematic error due to the variation of fragmentation parameters.

sample composition including all effects that stem from muon identification, branching ratios and the description of the transverse momentum spectrum. Second, there is the opposite side where the jet charge Q^{oppo} is computed. Here the effects of secondary interaction in matter affecting the charge spectrum have to be considered. The Monte Carlo model parameters which define the fragmentation process and thus the momentum spectrum entering the charge sum, were also investigated.

Systematic Error: Lepton Sample Composition

The sample composition was checked by varying the binning in P_T including different values for the cuts on minimum and maximum of the lepton total and transverse momentum. The results of these tests can be found in table 6.

In addition, other P_T definitions – P_T relative to the LUCLUS axis, P_T with respect to the jet thrust, P_T relative to the sphericity axis – were used to explore the b purity of the sample, and gave consistent results. These P_T definitions give slightly lower b purity but as a cross-check of the Monte Carlo description the final result should, and did, remain stable.

Finally, each lepton class in the sample was given a modified weight in order to see how a variation of the coefficients $a^{(i)}_{class}$ affects the result. The outcome of this study is listed in table 7.

The total systematic error due to these uncertainties in the lepton sample was calculated to be

$$\text{systematic error}: \ \Delta\overline{\chi}(\text{lepton sample}) = ^{+0.010}_{-0.007} \ . \tag{11}$$

Systematic Error: Fragmentation

Here the simulation of the inclusive charged momentum spectrum of $Z^0 \to b\bar{b}$ events was varied starting from the DELPHI Monte Carlo tuning which was obtained from the study of various standard observables of jets.

A powerful parameter to check whether different parts of the spectrum are over- or under-estimated is the exponent in the charge sum, since it gives different relative weight to soft and hard tracks. The parameter κ was varied between 0.3 and 1.0 and the change in the results was $\Delta\overline{\chi} = ^{+0.007}_{-0.002}$. As an additional cross-check the minimal momentum cut for tracks to enter the charge sum was changed between 0.1 GeV/c and 2.0 GeV/c and a variation of $\Delta\overline{\chi} = ^{+0.006}_{-0.002}$ was observed.

The impact of the longitudinal fragmentation function on the result was studied by the varying Peterson's $\epsilon_{b,c}$ using a weighting technique. This allowed us to compare the Monte Carlo description to the muon spectrum in the data (P and P_T) and determine an appropriate range of variation as well as the systematic uncertainty on the mixing.

The strange quark suppression factor $x_{\frac{s}{u}}$ and the probability for baryon formation $f_{baryons}$ affect the primary hadrons formed in the fragmentation process. These parameters can be changed directly in the fit function, assuming the dominant effect of $x_{\frac{s}{u}}$ to be the change in the ratio of B_d^0 and B_s^0 mesons. The range of variation is motivated by the result given in reference [13].

Finally other important parameters of the JETSET program were varied on generator level. Hadronic Z^0 decays were produced until at least 160000 leptons matching the requirements on P and P_T were detected. The change in the values of $< Q^{oppo} >$ obtained for the five b-jet classes and for the background classes (except misidentified hadrons) when compared to the results produced with the original parameter setting was determined. This set of systematic shifts was added to the corresponding Monte Carlo results of the full detector simulation which serve as input to the fitting of eqn. 6. Then the fit to the data was performed with the shifted Monte Carlo input numbers.

The evolution of the strong coupling constant during the parton-shower cascade is governed by Λ_{PS}^{QCD}. Different spin-states (vector or pseudoscalar mesons) are formed and the Gaussian transverse momentum distribution has a width of σ_{P_T}. The intervals in which the parameters were varied are chosen according to the tunings in [14] (Λ_{QCD}) or represent symmetrical variations around the defaults (σ_{P_T}, vector meson fraction). The fragmentation process stops if the invariant mass of the remaining unfragmented system is less than M_{frag}. The lower limit of M_{frag} is taken to be safely above the lightest hadron masses and the upper limit comes from the fit to DELPHI data. The results are displayed in table 8.

The total systematic error due to the fragmentation model is computed from the quadratic sum of the entries in table 8 and the larger value from the direct checks (ie. changing the exponent κ)

$$\text{systematic error : } \Delta\overline{\chi}(\text{fragmentation}) = ^{+0.014}_{-0.009} \, . \tag{12}$$

Also the definition of a hadronic event was changed. The requirement for the minimum number of charged tracks in the event was increased to 8 and an additional cut on the total momentum balance (20.0 GeV/c) was applied. The result was $\overline{\chi} = 0.145 \pm 0.015$. In comparison to the final result in eqn. 10 the error due to event selection is assigned to be $\Delta\overline{\chi} = \pm 0.001$.

The total systematic error is the quadratic sum of the two categories mentioned above plus the error due to the event selection criteria

$$\text{systematic error : } \Delta\overline{\chi}(\text{total}) = ^{+0.017}_{-0.011} \, . \tag{13}$$

Conclusion

The analysis of Z^0 decays from 1991 and 1992 DELPHI data with muon identification yields 46497 hadronic events with a muon in the momentum range $3.0 - 35.0$ GeV/c with transverse momentum between 0.5 GeV/c and 7.5 GeV/c, defined with respect to the momentum sum of the particles in the jet disregarding the muon itself.

A fit of the Monte Carlo expectation to the average value of the momentum weighted charge sum Q^{oppo} in different bins of transverse lepton momentum results in

$$\overline{\chi} = f_d \cdot \chi_d + f_s \cdot 0.9 \cdot \chi_s \quad = \quad 0.144 \pm 0.014 \ (stat.)^{+0.017}_{-0.011}(syst.). \tag{14}$$

The error is dominated by the systematic error of the Monte Carlo model which is mainly caused by the uncertainty of the tuning of the fragmentation parameters.

Although this analysis cannot discriminate between the B^0_d and B^0_s mixing, it nevertheless measures the B^0 mixing in an event sample which is inaccessible to the dilepton method. The combined measurements on the $\Upsilon(4S)$ [15], which are sensitive only to the B^0_d mixing, can be displayed as a horizontal band in the $\chi_s - \chi_d$ plane. The result of the present letter appears as a second band with negative slope. Assuming that the bands correspond to independent Gaussian probability densities, the log likelihood of the common density is the sum of the contributions of the two bands. The common likelihood of both results allows to set a limit on χ_s,

$$\chi_s > 0.31 \ (95\% \ c.l.). \tag{15}$$

The complete likelihood contour in the (χ_d, χ_s) plane is shown in figure 7.

Acknowledgements

We are greatly indebted to our technical collaborators and to the funding agencies for their support in building and operating the DELPHI detector, and to the members of the CERN-SL Division for the excellent performance of the LEP collider.

References

[1] C. Albajar et al., (UA1 Collaboration), Phys. Lett. **B 186** (1987) 247,
H. Albrecht et al. (ARGUS Collaboration), Phys.Lett. **B 192** (1987) 245.

[2] A. Pais and S.B. Treiman, Phys. Rev. **D 12** (1975) 2744,
L.B. Okun, V.I. Zakharov and B.M. Pontecorvo Nuovo Cimento Lett. (1975) 218,
J. Ellis, M.K. Gaillard and D.V. Nanopoulos, Nucl.Phys. **B 109** (1976) 213.

[3] M. Kobayashi and K. Maskawa, Progr. Theor. Phys. **49** (1973) 652.

[4] M. Akwary et al. (OPAL Collaboration), Phys. Lett. **B 236** (1990) 364,
D. Decamp et al. (ALEPH Collaboration), Phys. Lett. **B 258** (1991) 236,
B. Adeva et al. (L3 Collaboration), Phys. Lett. **B 288** (1992) 395,
P. Abreu et al. (DELPHI Collaboration), Phys. Lett. **B 301** (1993) 145.

[5] D. Decamp et al. (ALEPH Collaboration), Phys. Lett. **B 284** (1992) 177.

[6] P. Abreu et al. (DELPHI Collaboration), Nucl. Instr. Methods **A 303** (1991) 233.

[7] N. Crosland, G. Wilkinson and P. Kluit, EMMASS, DELPHI Note 92-17.

[8] T. Sjöstrand and M. Bengtson, Comput. Phys. Commun. **43** (1987) 367,
T. Sjöstrand in CERN-89-08, Vol. 3, 143.

[9] N. Isgur, D. Scora, B. Grinstein, and M. B. Wise, Phys. Rev. **D 39** (1989) 799.

[10] M. Wirbel, B. Stech, M. Bauer, Z. Phys. **C 29** (1985) 637,
M. Bauer, B. Stech, M. Wirbel, Z. Phys **C 34** (1987) 103.

[11] H. Albrecht et al. (ARGUS Collaboration), Phys. Lett. **B 249** (1990) 359,
J. C. Gabriel, Dissertation, Heidelberg 1989, IHEP-HD/89-1.

[12] P. Roudeau, plenary session talk at the *Joint International Lepton-Photon-Symposium and Europhysics Conf.*, Geneva 1991, eds. S. Hegarty, K. Potter and E. Quercigh, World Scientific, Singapore 1992.

[13] P. Abreu et al. (DELPHI Collaboration), Phys. Lett. **B 275** (1992) 231.

[14] W. Braunschweig et al. (TASSO Collaboration), Z. Phys. **C 41** (1988) 359,
A. Peterson et al. (MARK II Collaboration), Phys. Rev. **D 37** (1988) 1.

[15] H. Albrecht et al. (ARGUS Collaboration), Z. Phys. **C 55** (1992) 357,
M. Artuso et al., (CLEO Collaboration), Phys. Rev. Lett. **62** (1989) 2233.

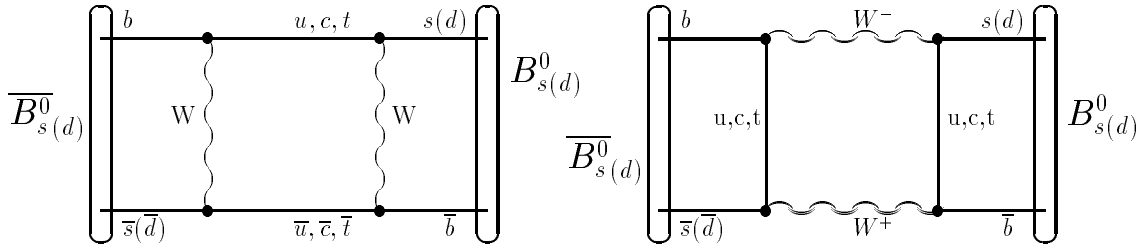

Figure 1: Feynman graphs for $\overline{B^0}$-B^0 transitions.

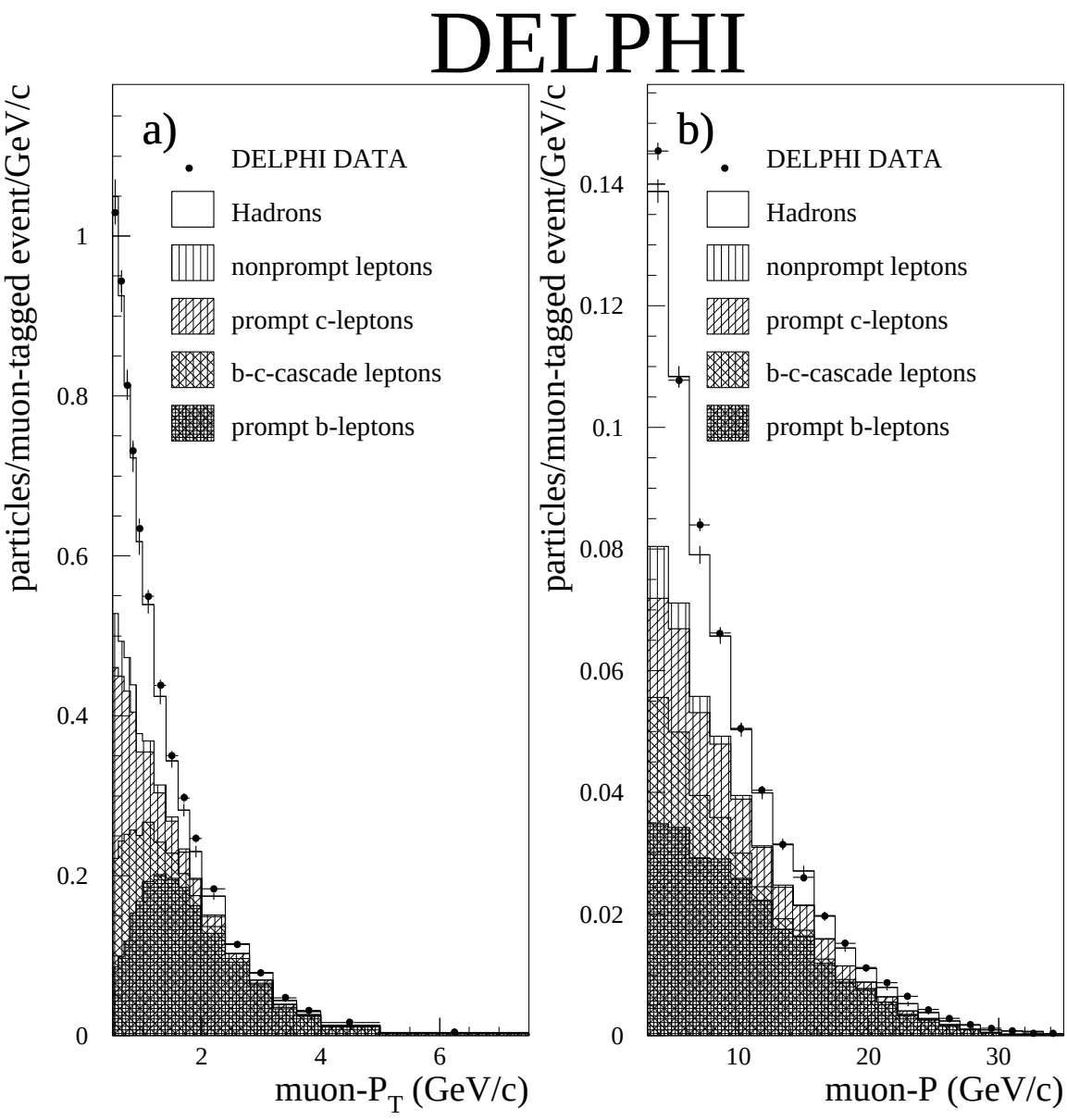

Figure 2: Normalised muon spectra; a) transverse momentum, b) absolute momentum; points: DELPHI data, histograms: Monte Carlo expectation.

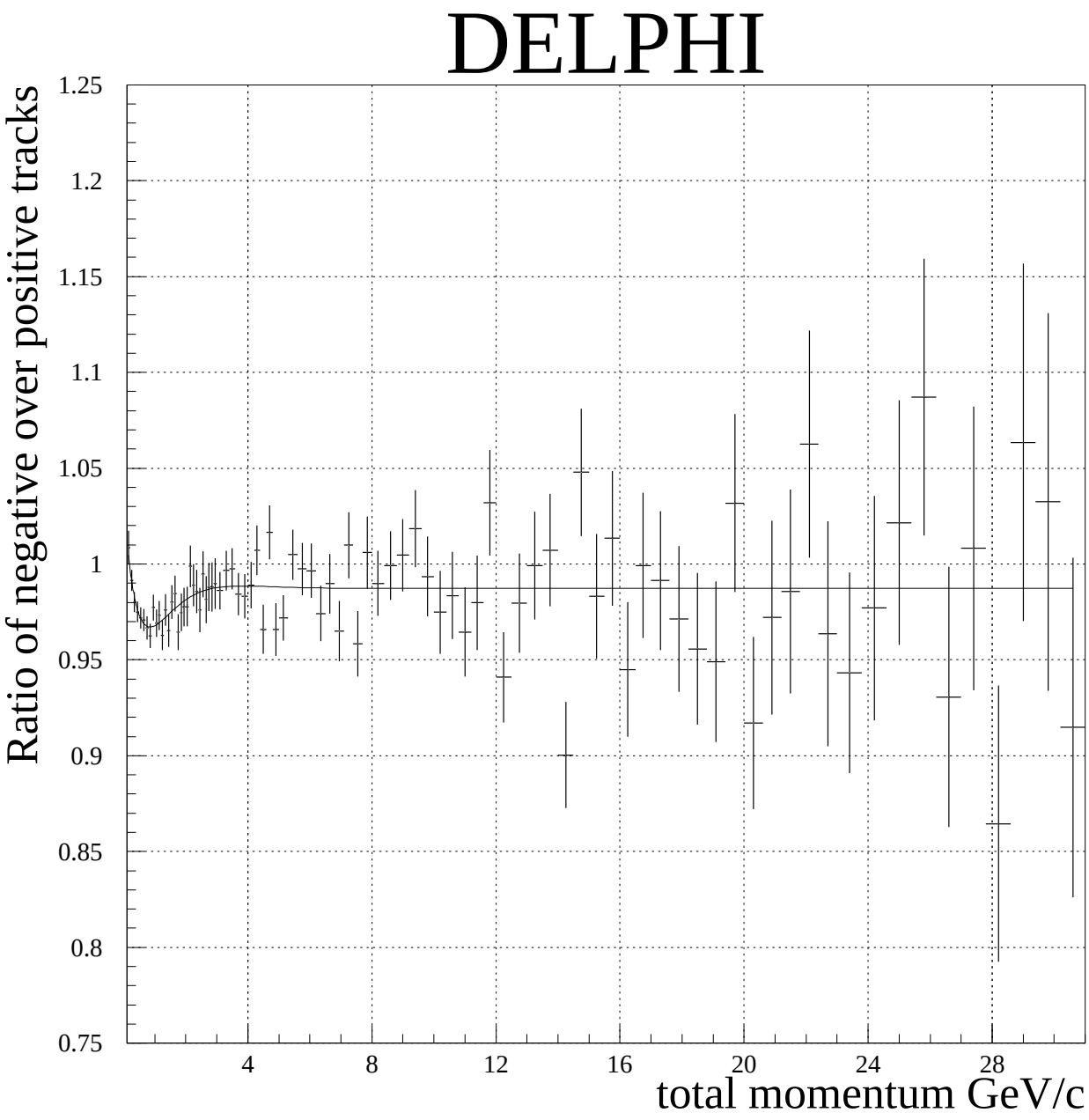

Figure 3: DELPHI data: Ratio of negative to positive charged particles in the data as function of momentum p, together with the parametrisation $f(p)$ (cf. in the text).

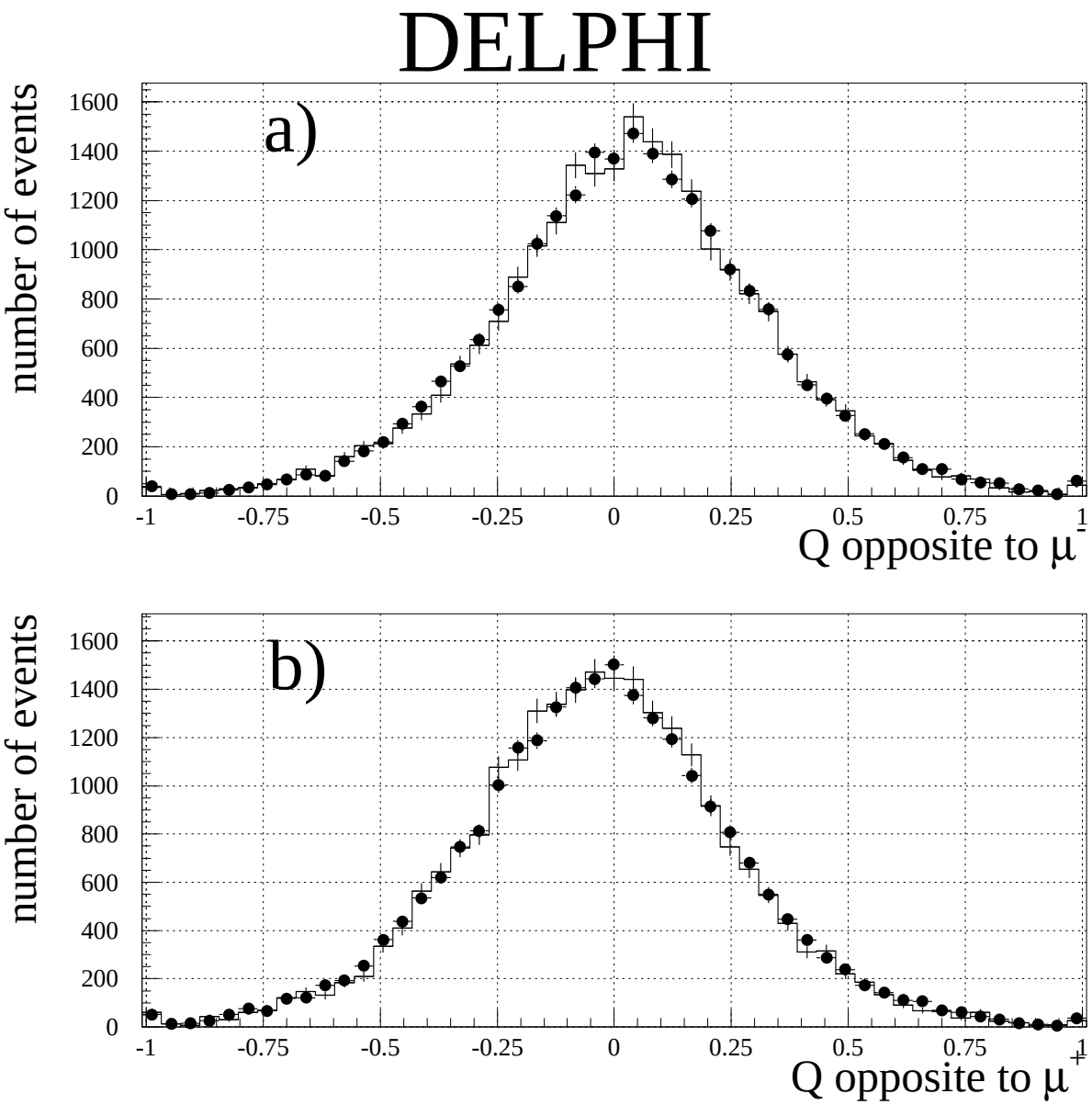

Figure 4: The jet charge Q^{oppo} opposite to the muon a) for negative and b) positive muons. A value of $\kappa = 0.6$ is used. The mean values are a) $Q^{oppo} = 0.0322 \pm 0.0019$ and b) $Q^{oppo} - 0.0318 \pm 0.0019$. The Monte Carlo expectation for $\chi_s = 0.49$ and $\chi_d = 0.19$ is given as histogram. This distribution is sensitive to mixing.

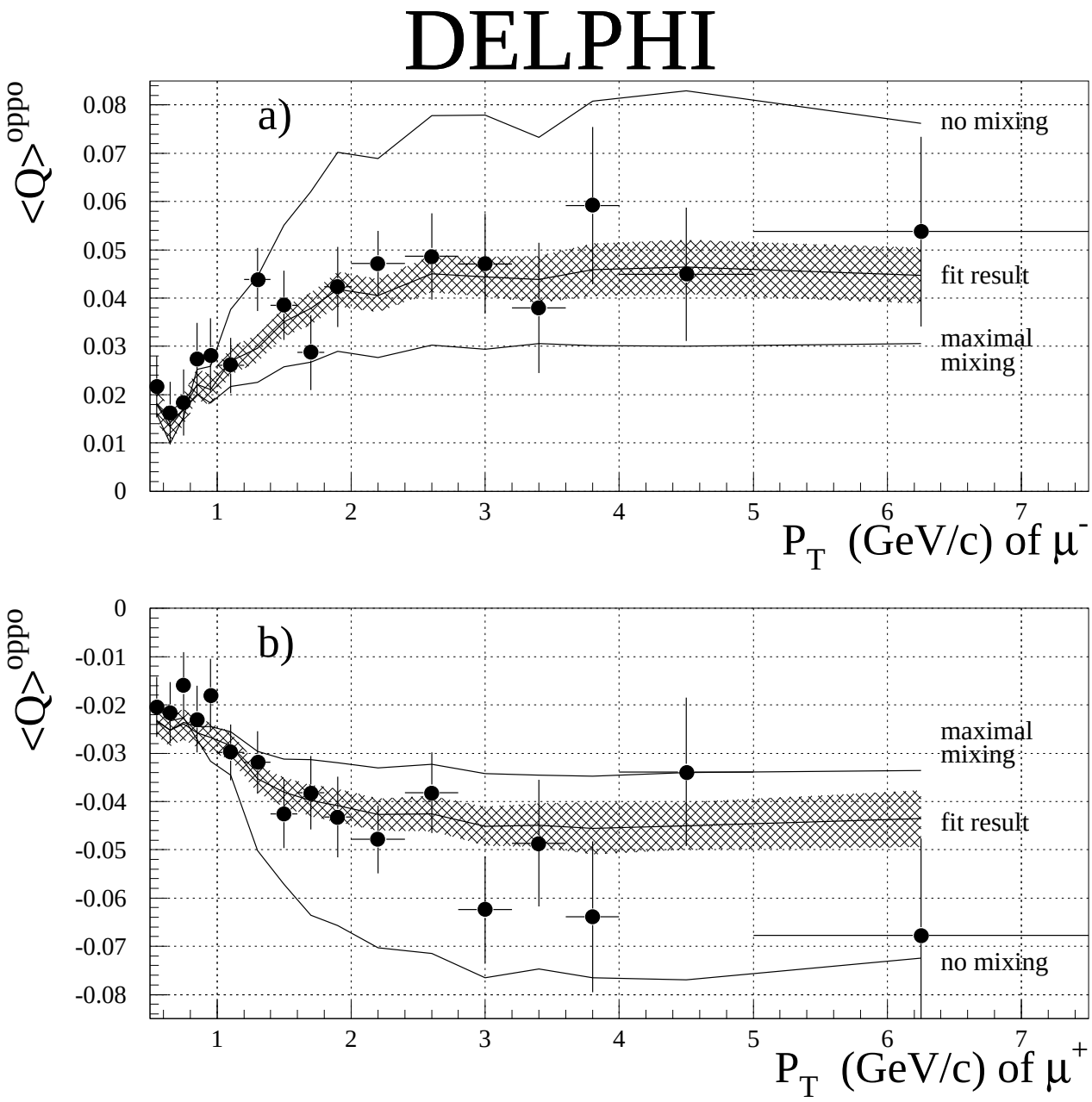

Figure 5: The mean jet charge opposite to the muon Q^{oppo} for a) negative and b) positive muons, as a function of the transverse momentum of the muon. The lines indicate the model expectation for no mixing ($\chi_d = \chi_s = 0.0$), full mixing ($\chi_d = \chi_s = 0.5$) and the fit result displayed as a band showing the statistical uncertainty of the Monte Carlo model.

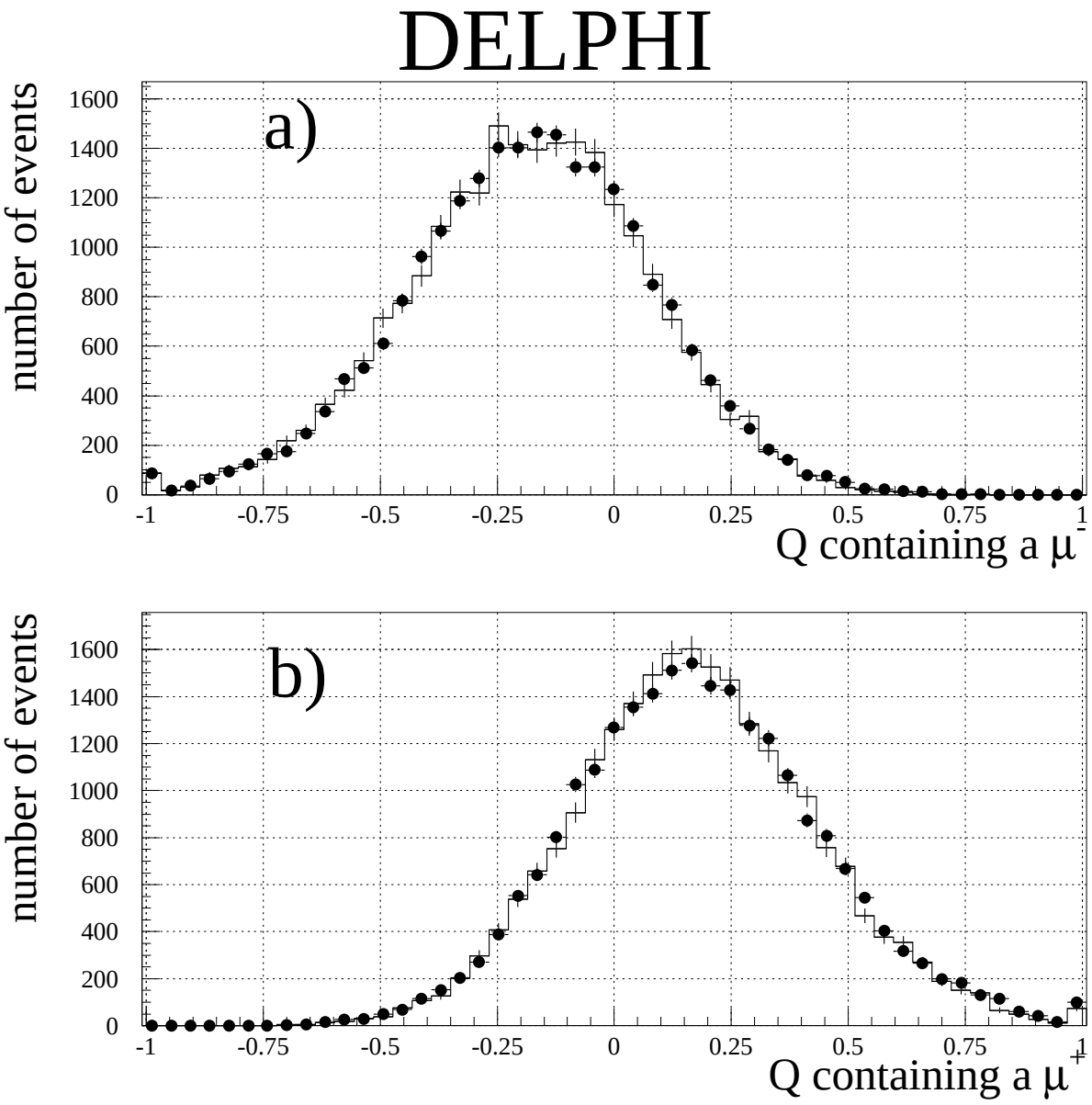

Figure 6: The jet charge Q^{same} containing the muon a) for negative and b) positive muons. A value of $\kappa = 0.6$ is used. The Monte Carlo expectation is given as histogram. This distribution is nearly not affected by mixing.

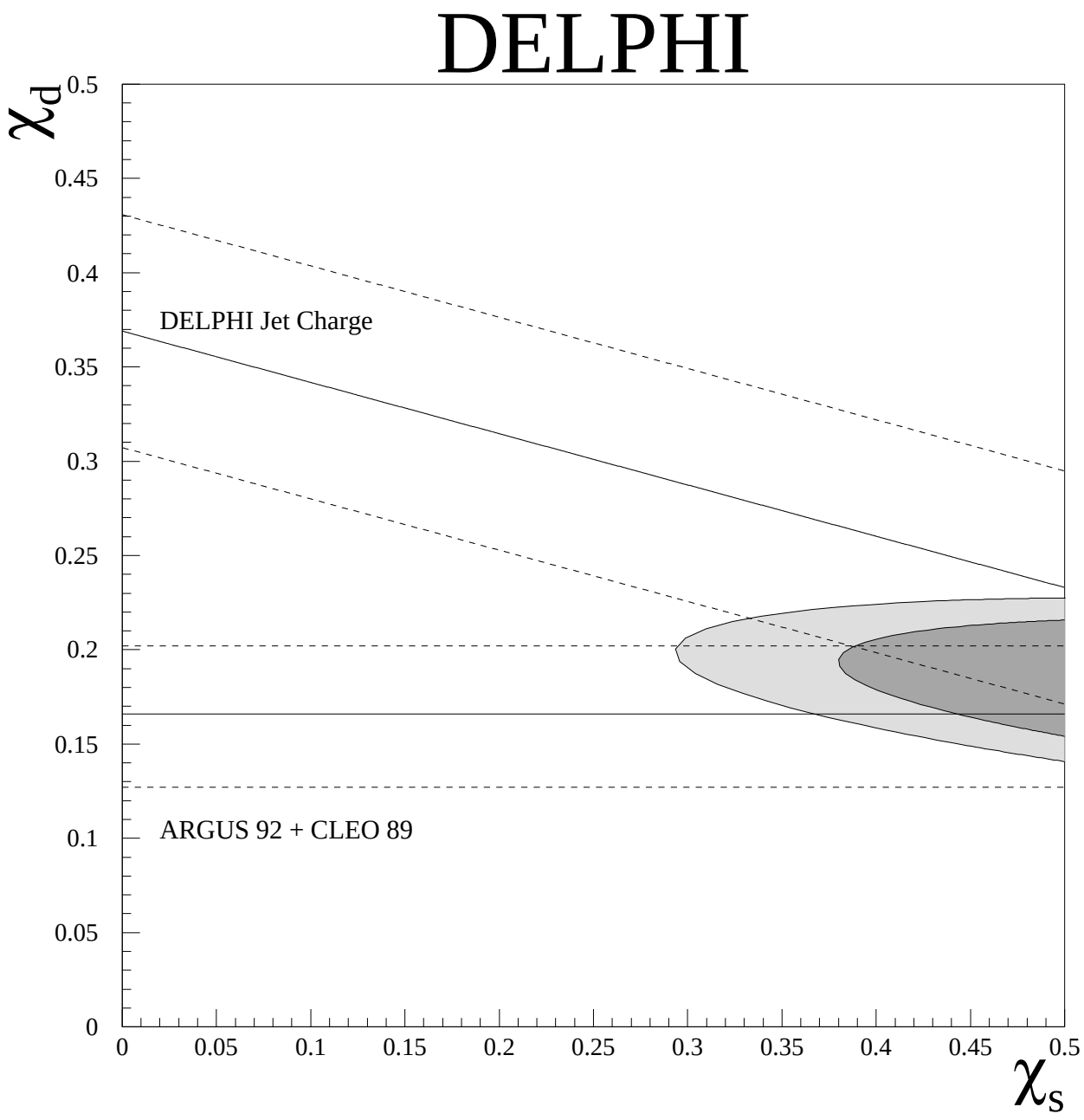

Figure 7: The fit result χ_d for various assumptions on χ_s. The dashed lines indicate the 1σ contour of the total error. The result from the $\Upsilon(4S)$ experiments appear as horizontal lines. From the construction of a common likelihood function, assuming Gaussian errors, the 1σ and 2σ confidence areas are drawn.